Exact time-dependent evolution of electron-velocity distribution functions in a gas using the Boltzmann equation

P. J. Drallos and J. M. Wadehra
Department of Physics and Astronomy, Wayne State University, Detroit, Michigan 48202
(Received 22 March 1989)

A numerical technique, starting from the Boltzmann equation, for obtaining the time-dependent behavior of the electron-velocity distribution function in a gas is presented. A unique feature of this technique is that, unlike previously used procedures, it does not make use of *any* expansion of the distribution function. This allows the full anisotropy of the distribution function to be included in the solution. Furthermore, the problem associated with multiterm-expansion techniques of choosing a sufficient number of terms for convergence is completely avoided. The distribution function obtained by the present method is exact and, in principle, contains all of the expansion terms of the previous procedures. Details of the algorithm, including stability conditions, treatment of the boundaries, and evaluation of the collision integrals, are presented. This technique has been applied for obtaining the time-dependent behavior of electron swarms in gaseous argon and neon for various values of E/N (the ratio of the applied uniform dc field to the gas density), and the corresponding results are presented.

I. INTRODUCTION

The electron-velocity distribution function (EVDF) is fundamentally important in virtually all aspects of gaseous electronics. The EVDF provides a statistical description of the motion of all of the electrons in an electron swarm. The motion of the electrons in the swarm is affected by externally applied electric and magnetic fields, and by collisions of the electrons with the particles of the ambient gas. These external forces and collisions cause time-dependent changes in the EVDF. Stating this process mathematically, let $f(\mathbf{v},t)$ represent the electron-velocity distribution function at a velocity $\mathbf{v}$, and at a particular time t. Then, at some later time $t+\Delta t$, the EVDF can be described very simply by

$$f(\mathbf{v}+\Delta\mathbf{v},t+\Delta t)=f(\mathbf{v},t)+R(\mathbf{v},t)\Delta t \ . \tag{1}$$

Here, $\Delta\mathbf{v}=\mathbf{a}\Delta t$, with $\mathbf{a}$ as the acceleration of the electrons due to the externally applied forces. $R(\mathbf{v},t)\Delta t$ is the collision term which represents the net change in $f(\mathbf{v},t)$ during the time increment Δt due to all possible collision processes between the electrons and the gas particles. Now, if we expand Eq. (1) to first order in Δt, and then take the limit as Δt goes to zero, the spatially independent Boltzmann equation is immediately obtained:

$$\frac{\partial f(\mathbf{v},t)}{\partial t}+\mathbf{a}\cdot\nabla_v f(\mathbf{v},t)=R(\mathbf{v},t) \ . \tag{2}$$

It is thus clear that the physical content of the Boltzmann equation (2) is entirely equivalent to that of the difference equation (1). Knowledge of the EVDF is usually gained by solution of the Boltzmann equation and, to this end, many techniques for its solution have been developed.

Traditionally, the techniques used for solving the Boltzmann equation for an equilibrium electron-velocity distribution function have involved expansion, usually in the Legendre polynomials, of the distribution function as follows:

$$f(\mathbf{v},t)=\sum_{n=0}^{\infty} f_n(v,t)P_n(\theta) \ . \tag{3}$$

Often, only the first two terms in the expansion, containing f_0 and f_1, are retained, and the time derivative of the distribution function in the Boltzmann equation is set to zero to correspond to the equilibrium situation. The resulting coupled time-independent equations can then be solved for f_0 and f_1 using standard numerical methods. The two-term expansion method, however, breaks down[1] under situations of large E/N (the ratio of the applied uniform dc electric field to the gas density) or for cases in which the inelastic scattering cross sections are comparable in magnitude to the elastic cross sections. The shortcomings of the two-term expansion can, in principle, be overcome by retaining more terms in the Legendre expansion of the distribution function. These multiterm methods, however, have their own drawbacks. As more terms in the expansion are kept, the computational complexity increases rapidly. Furthermore, cross sections which have been adjusted to reproduce experimental swarm parameters in a two-term expansion calculation do not yield the same EVDF or the corresponding swarm parameters when used in a multiterm expansion calculation and vice versa. Clearly, it would be desirable to have a procedure, as described below, which can provide the equilibrium EVDF without involving any expansion of the distribution function. Such a procedure, which incorporates a finite-difference technique, was developed by Tagashira and co-workers.[2] In their procedure, the distribution function was expanded to second order in time using a standard Taylor series. The various time derivatives of $f(\mathbf{v},t)$ were evaluated by direct substitution from

the Boltzmann equation, namely,

$$f(\mathbf{v},t+\Delta t)=f(\mathbf{v},t)+\frac{\partial f(\mathbf{v},t)}{\partial t}\Delta t+O((\Delta t)^2)$$
$$=f(\mathbf{v},t)+[-\mathbf{a}\cdot\nabla_v f(\mathbf{v},t)+R(\mathbf{v},t)]\Delta t$$
$$+O((\Delta t)^2)\ . \tag{4}$$

Tagashira and co-workers chose to evaluate the distribution function of Eq. (4) in spherical coordinates in the velocity space, that is, f was stored as a v-θ array, simply because the evaluation of the collision term $R(\mathbf{v},t)$ is most convenient in spherical coordinates. Evaluation of the $\mathbf{a}\cdot\nabla_v$ term then involved derivatives of f with respect to v and θ. These derivatives, which had to be taken numerically by a finite-difference procedure, are prone to instability. It was in order to alleviate this instability that Tagashira and co-workers had to retain some of the terms proportional to $(\Delta t)^2$ in the Taylor-series expansion of Eq. (4). In a previous paper,[3] we briefly described a finite-difference algorithm for determining the exact time-dependent behavior of electron-velocity distribution functions. A unique feature of our algorithm is that it does not require numerical evaluation of *any* derivatives, nor does it make use of any term expansions of the distribution function in terms of Legendre functions. The present paper will provide details of the procedure, such as the explicit form and evaluation of the collision integrals, conditions of numerical stability, treatment of the numerical boundaries, and techniques for implementing the conditions of numerical stability. We will also present results of the application of this procedure to electron swarms in argon and in neon for various values of E/N.

In the present solution, the following finite-difference equation in Cartesian coordinates for the electron-velocity distribution function is evaluated

$$f(v_x,v_y,v_z+\Delta v_z,t+\Delta t)$$
$$=f(v_x,v_y,v_z,t)+R(v_x,v_y,v_z,t)\Delta t\ . \tag{5}$$

Equation (5) can be obtained directly from Eq. (1), which is equivalent, in its physical content, to the Boltzmann equation (2). Until the collision terms $R(\mathbf{v},t)$ are known, however, Eq. (5) is of little practical use. So, before proceeding any further, we will explicitly define the collision terms $R(\mathbf{v},t)$ and outline procedures for their evaluation.

II. COLLISION TERMS

In order to derive a very general expression for the collision term we will assume an ambient gas of constant density interacting with a spatially homogeneous swarm of projectiles of arbitrary mass (for example, either electrons, positrons, protons, or ions). A general expression for the collision term in Eq. (5) can be written[4]

$$R(\mathbf{v},t)=\sum_p (N/v^2)\int_0^\infty v_p^2 dv_p \int_0^\pi \sin\psi\, d\psi \int_0^{2\pi} d\alpha\, v_p f(\mathbf{v}_p,t)\sigma_p(v_p,\psi)\delta(v-g_p(v_p,\psi))-Nvf(\mathbf{v},t)\sigma_T(v) \tag{6}$$

where $\sigma_p(v_p,\psi)$ is the differential scattering cross section for the pth (p = elastic, excitation, ionization, etc.) collision process, and $\sigma_T(v)$ is the integrated total cross section for all collision processes. The function $g_p(v_p,\psi)$ is defined by the equation

$$v=g_p(v_p,\psi)\ , \tag{7}$$

which relates, via the energy-conserving δ function, the initial speed v_p to the final speed v for the pth collision process. The integral terms in Eq. (6) represent the rate at which the projectile particles are scattered into a velocity-space-volume element d^3v located about $\mathbf{v}$ due to the pth scattering process and will be denoted by $R^+(\mathbf{v},t)$. The last term in Eq. (6) represents the rate at which the projectile particles are scattered out of d^3v about $\mathbf{v}$ due to all possible collision processes, and will be denoted by $R_T^-(\mathbf{v},t)$. Thus

$$R(\mathbf{v},t)=\sum_p R_p^+(\mathbf{v},t)-R_T^-(\mathbf{v},t)\ .$$

The differential velocity-space volume elements in Eq. (6) are defined in Fig. 1 and by the following relations:

$$d^3v=v^2dv\sin(\theta)d\theta\,d\phi\ , \tag{8a}$$

$$d^3v_p=v_p^2dv_p\sin(\theta_p)d\theta_p d\phi_p=v_p^2dv_p\sin(\psi)d\psi\,d\alpha\ , \tag{8b}$$

so that the direction of $\mathbf{v}_p$ can be specified, depending on the convenience, with respect to either $\mathbf{z}$ or $\mathbf{v}$. These two possible specifications of $\mathbf{v}_p$ lead to the following relationships among various angles:

$$\mathbf{v}=\mathbf{v}(v,\theta)\ , \tag{9a}$$

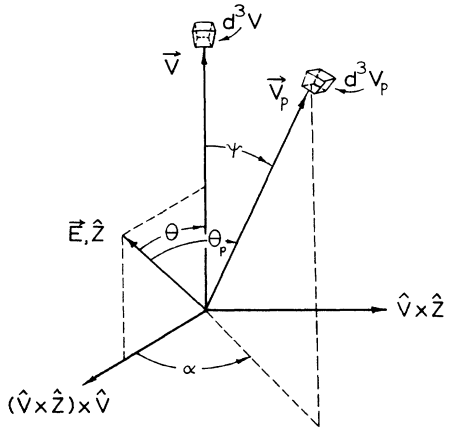

FIG. 1. Geometry used in the derivation of the collision terms. $\mathbf{v}$ the $\mathbf{v}_p$ denote the final and initial velocities, respectively, and ψ is the scattering angle.

$$\cos(\theta_p)=\sin(\theta)\sin(\psi)\cos(\alpha)+\cos(\theta)\cos(\psi) , \tag{9b}$$

$$\mathbf{v}_p=\mathbf{v}_p(v_p,\theta_p)=\mathbf{v}_p(v_p,\theta,\psi,\alpha) , \tag{9c}$$

and finally,

$$f(\mathbf{v}_p,t)=f(v_p,\theta_p,t)=f(v_p,\theta,\psi,\alpha,t) . \tag{9d}$$

In order to evaluate Eq. (6) the function $g_p(v_p,\psi)$ must be specified for various collision processes. For *elastic* collisions ($p=e$), straightforward kinematics yields

$$v=v_e q(\psi)=g_e(v_e,\psi) , \tag{10a}$$

where $q(\psi)$ is the following function:

$$q(\psi)=[(1-\mu^2)^{1/2}+\mu\cos\psi]/(1+\mu) . \tag{10b}$$

Here, μ is the ratio of the mass m of the projectile and the mass M of the gas particle, that is, $\mu=m/M$. For the case in which the projectile is either an electron or a positron ($\mu \ll 1$), $q(\psi)$ can be simplified to

$$q(\psi)=[1-\mu(1-\cos\psi)] . \tag{10c}$$

For *inelastic* collisions ($p=i$) the energy-conserving expression for g_p is

$$v=(v_i^2-2\xi/m)^{1/2}=g_i(v_i) , \tag{11}$$

which does not depend on the angle ψ. ξ is the energy loss associated with the inelastic process. Performing the radial v_p integrations to eliminate the Dirac δ functions in Eq. (6), one is left with a two-dimensional angular integral over ψ and α. Because of the δ function, v_p in the integrand, which includes the distribution function f and the collision cross section σ_p, is replaced by $v/q(\psi)$ (for the elastic part) or by $(v^2+2\xi/m)^{1/2}$ (for the inelastic part). For brevity in writing and in accordance with Eqs. (10) and (11), we replace, in the resulting angular integrals, $v/q(\psi)$ and $(v^2+2\xi/m)^{1/2}$ with v_e and v_i, respectively, so that the final expression for the collision term looks like

$$\begin{aligned} R(\mathbf{v},t)= & N\int_0^{\pi}\frac{v_e^4}{v^3}\sigma_e(v_e,\psi)\sin\psi\,d\psi\int_0^{2\pi}f(\mathbf{v}_e,t)d\alpha \\ & +\sum_i N\int_0^{\pi}\frac{v_i^2}{v}\sigma_i(v_i,\psi)\sin\psi\,d\psi \\ & \times\int_0^{2\pi}f(\mathbf{v}_i,t)d\alpha-Nvf(\mathbf{v},t)\sigma_T(v) . \end{aligned} \tag{12a}$$

So far, the collision integral is valid for any type of projectile except that the term corresponding to the ionization process has to be treated slightly differently when the projectile is an electron. When ionization is considered, the final energy of both the incident electron and the free electron that is produced via the ionization process must be properly accounted for. To this end, an electron-energy partition ratio $\Delta/(1-\Delta)$ is used, which denotes the ratio of the available energy that goes to each of the two electrons (labeled 1 and 2 below). The integral that represents the rate at which electrons scatter due to the ionization process, into the velocity space element d^3v about (v,θ), then has two parts:

$$\begin{aligned} & R^{+}_{\text{ion},1}(v,\theta)+R^{+}_{\text{ion},2}(v,\theta) \\ & =\frac{N}{\Delta}\int_0^{\pi}\frac{v_1^2}{v}\sigma_{\text{ion}}(v_1,\psi)\sin\psi\,d\psi\int_0^{2\pi}f(\mathbf{v}_1,t)d\alpha \\ & \quad+\frac{N}{1-\Delta}\int_0^{\pi}\frac{v_2^2}{v}\sigma_{\text{ion}}(v_2,\psi)\sin\psi\,d\psi\int_0^{2\pi}f(\mathbf{v}_2,t)d\alpha , \end{aligned} \tag{12b}$$

where $v_1=(2\xi/m+v^2/\Delta)^{1/2}$ and $v_2=[2\xi/m+v^2/(1-\Delta)]^{1/2}$. These two terms correspond to two different ionization events in which electrons of initial speeds v_1 and v_2 ionize gas particles. One of the two electrons [having energy ratio $\Delta/(1-\Delta)$] resulting from each of these two ionization events has speed v.

In evaluating Eqs. (6) or (12), proper account must be taken of the vector nature of $\mathbf{v}$ and $\mathbf{v}_p$. Although the distribution function is symmetric about the axis parallel to the electric field (the $\mathbf{z}$ axis), the polar axis of the integrals over a solid angle (ψ,α) is tilted with respect to $\mathbf{z}$ and cannot take advantage of the symmetry.

The surface over which the distribution function in the *elastic* part of Eq. (12a) is evaluated for angular integration is represented graphically in Fig. 2. Note that, because v_e depends on ψ, the surface is not a perfect sphere but an "egg-shaped" surface with azimuthal symmetry about $\mathbf{v}$. More specifically, such a surface is realized by the tracing of the tip of a vector whose length increases continuously as the polar angle is varied from one pole ($\psi=0$) to the other pole ($\psi=\pi$), but the length of the vector remains fixed as the azimuthal angle α is varied, for a given ψ, from 0 to 2π. The deviation of this surface from a perfect sphere is related, from Eq. (10), to the mass ratio μ. If the projectile particles are electrons or positrons the surface is very nearly a sphere, and very little difference was found on simply replacing v_e by v in Eq. (12a). However, in order to keep the analysis more general and not limit the distribution functions to only those

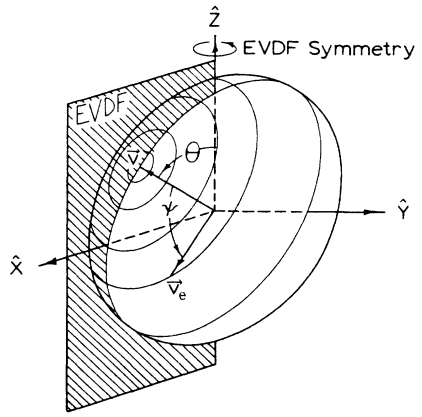

FIG. 2. Surface over which the elastic component of the collision term is evaluated. θ is the polar angle about $\mathbf{z}$, and ψ is the polar angle about $\mathbf{v}$.

of electrons or positrons, we will not make any assumptions about the relative masses of the gas molecules and the projectiles. Nevertheless, Eq. (12a) remains valid in all possible cases including the ones in which the projectile particles are more massive, such as protons or ions, for which the distortion and tilt of the surface would become very important.

Often, the differential scattering cross sections are not sufficiently available to cover all angles and energies for each scattering process in the system of interest. Integrated cross sections, however, can usually be found and may be the only alternative. In this case, or in the cases in which the scattering is not strongly dependent on angle, we may make the approximation of isotropic scattering (σ does not depend on ψ). For isotropic elastic scattering we replace the differential elastic scattering cross section $\sigma_e(v_e,\psi)$ with $\sigma_e(v_e)/4\pi$, where $\sigma_e(v_e)$ is the integrated elastic scattering cross section. Doing this, the elastic part of Eq. (12) can be rewritten as

$$R_e^+(\mathbf{v},t)=\frac{N}{4\pi v^3}\int_0^{\pi} v_e^4\sigma_e(v_e)\sin\psi\, d\psi\int_0^{2\pi} f(\mathbf{v}_e,t)d\alpha\ . \tag{13}$$

If we assume isotropic *inelastic* scattering, then the differential scattering cross section for the ith scattering process $\sigma_i(v_i,\psi)$ can be replaced by $\sigma_i(v_i)/4\pi$, where $\sigma_i(v_i)$ is the integrated cross section for the ith inelastic process. Also, since v_i does not depend on the scattering angle, the surface of integration is spherical with a constant radius v_i, and the terms containing v_i can be taken outside of the angular integral. We can then write

$$R_i^+(\mathbf{v},t)=\frac{Nv_i^2}{4\pi v}\sigma_i(v_i)\int_0^{\pi}\sin\psi\, d\psi\int_0^{2\pi} f(\mathbf{v}_i,t)d\alpha \tag{14a}$$

$$=\frac{Nv_i^2}{4\pi v}\sigma_i(v_i)\int_0^{\pi}\sin\theta_i d\theta_i\int_0^{2\pi} f(\mathbf{v}_i,t)d\phi_i \tag{14b}$$

$$=\frac{Nv_i^2}{2v}\sigma_i(v_i)\int_0^{\pi} f(v_i,\theta_i,t)\sin\theta_i d\theta_i\ . \tag{14c}$$

In going from Eq. (14a) to (14b) we have made use of the fact that the integral is independent of the choice of polar axis and we have chosen the z axis (which is the axis of symmetry for the EVDF) as the polar axis, so that the ϕ_i integration becomes trivial [see Eq. (8b)].

Another problem that must be considered in the evaluation of Eq. (12a) is that f is stored in a rectangular array (in the x-z plane) and has rectangular boundaries, but the surfaces of integration in the R^+ terms are nonrectangular and sometimes lie outside of the region in which f is known. To handle this problem, an extrapolation procedure has to be devised. Regrettably, extrapolations are a risky business, and one can only hope that the relevant numerical errors will be small. What we did was to set up the initial ($t=0$) Maxwellian distribution of projectiles (electrons in our actual calculations) so that the values of the distribution function near the boundaries were less than 10^{-5} of the peak value so that the boundary contributions would be small. Then we assumed that the behavior in the high-velocity regions (near the boundaries and beyond) remained essentially Maxwellian at all later times. Based on the shape of the distribution function near but inside the boundary, we extrapolated the distribution function using the simple recursion relation $f(v+2\Delta v)=[f^2(v+\Delta v)/f(v)]C$, where C is a constant that depends on Δv. This recursion relation follows from the assumed Maxwellian form of the distribution function near the boundary. The case $C=1$ corresponds to the logarithmic approximation for extrapolation used by previous investigators.[2] Several tests were made, by changing the boundaries, showing that the high-velocity tail of the numerically obtained distribution function conformed to this Maxwellian behavior, and that deviation was less than 1%.

III. METHOD OF SOLUTION

For the situation in which the external force on the projectiles (of charge q) is provided by a uniform dc electric field aligned in the **z** direction, the constant $\Delta v_z=(qE/m)\Delta t$, and Eq. (5) can be rewritten as

$$f(v_x,v_y,v_z+(qE/m)\Delta t,t+\Delta t)=f(v_x,v_y,v_z,t)+R(v_x,v_y,v_z,t)\Delta t\ . \tag{15}$$

Equation (15) is well suited for evaluation on a computer. Since there is axial symmetry around the z axis, f need only be stored as a function of v_z and v_x (or v_y) in such a way that the velocity increments Δv satisfy the relation $\Delta v=(qE/m)\Delta t$. Evaluation of f in Eq. (15) then merely involves a shifting of the two-dimensional array $f(v_x,v_z)$ along v_z at each time interval Δt, and then adding to each array element the corresponding collision term $R(v_x,v_z,t)\Delta t$. This shifting procedure accomplishes all the acceleration effects of the projectiles due to the electric field and is inherently immune to round-off error. Carrying out this procedure will require knowledge of the collision integrals for each v_x and v_z at time t. Evaluation of these integrals was described in Sec. II, and involves an integral over the polar angle θ (in velocity space) and thus requires a knowledge of the distribution function at various values of v and θ. This integration can be carried out, even though f is known only as a function of v_x and v_z, by simply interpolating $f(v_x,v_z)$ to get $f(v,\theta)$.

The algorithm for obtaining the time evolution of the velocity distribution function is as follows.

(i) Store an initial distribution function (for instance, a Maxwellian at $t=0$) in a two-dimensional array $f(v_x,v_z)$ such that $\Delta v=(qE/m)\Delta t$.

(ii) From the existing distribution function, evaluate the collision terms $R(v_x,v_z)$ for each v_x and v_z.

(iii) Multiply each of the collision terms by Δt and add to the corresponding distribution function array element $[f(v_x,v_z)\rightarrow f(v_x,v_z)+R(v_x,v_z)\Delta t]$.

(iv) Shift the resulting array along the v_z index $[f(v_x,v_z)\rightarrow f(v_x,v_z+\Delta v_z)]$ to obtain a new distribution function which corresponds to time $t+\Delta t$.

(v) Go to step (ii).

The procedure outlined in steps (ii)–(v) are repeated while various swarm parameters are calculated from the

distribution function obtained in step (iv) for each time cycle. Equilibrium is obtained when the swarm parameters cease to change in time.

IV. STABILITY CONDITIONS

In any numerical solution to a differential equation, stability is always a major consideration. The procedure of shifting the array elements along the v_z index accomplishes all of the acceleration effects due to the electric field and avoids the need to evaluate any derivatives numerically. This procedure in itself greatly enhances the numerical stability of the calculation; however, it is not in itself sufficient. One of the conditions of stability is a restatement of the so-called Courant-Friedrichs-Lewy[5] (CFL) condition and is simply

$$(a\Delta t)/\Delta v \leq 1 , \tag{16}$$

where $a = qE/m$ is, in this case, the acceleration of the projectiles due to the electric field **E**. Since f is stored so that its velocity increments satisfy $\Delta v = (qE/m)\Delta t$, Eq. (16) is always minimally satisfied as an *equality*. The calculation can satisfy Eq. (16) more strongly by choosing a smaller time increment $\Delta t'$, which is a proper fraction of Δt such that

$$\Delta t' = \Delta t/n, \quad \Delta \mathbf{v}' = \Delta \mathbf{v}/n , \tag{17}$$

while leaving a and Δv unchanged. Then Eq. (5) can be rewritten

$$\begin{aligned} f(\mathbf{v}+\Delta\mathbf{v}, t+\Delta t') &= f(\mathbf{v}+\Delta\mathbf{v}-\Delta\mathbf{v}', t) \\ &\quad + R(\mathbf{v}+\Delta\mathbf{v}-\Delta\mathbf{v}', t)\Delta t' \\ &= f(\mathbf{v}+\Delta\mathbf{v}(1-1/n), t) \\ &\quad + R(\mathbf{v}+\Delta\mathbf{v}(1-1/n), t)\Delta t' . \end{aligned} \tag{18}$$

A consequence of using a time step $\Delta t'$ smaller than $\Delta t = \Delta v m/(qE)$ is that the right-hand side of Eq. (18) calls for values of f and R from velocity-space locations which are not explicitly stored in the array. We can approximate Eq. (18) into a usable form with some simple linear interpolation of the f and R arrays from their stored values to obtain

$$\begin{aligned} &f(\mathbf{v}+\Delta\mathbf{v}, t+\Delta t') \\ &\quad = [(n-1)/n][f(\mathbf{v}+\Delta\mathbf{v}, t) + R(\mathbf{v}+\Delta\mathbf{v}, t)\Delta t'] \\ &\qquad + (1/n)[f(\mathbf{v}, t) + R(\mathbf{v}, t)\Delta t'] . \end{aligned} \tag{19}$$

The above procedure for rigorously implementing the CFL stability condition is represented graphically in Fig. 3.

Another condition for the numerical stability requires that each of the array elements of the distribution function f be larger than the corresponding array elements of the collision term. Restating algebraically,

$$f(\mathbf{v}, t)/[R(\mathbf{v}, t)\Delta t] > 1 . \tag{20}$$

This condition can be met by selecting Δt such that Eq. (20) is satisfied for all **v**. Experience has shown that the ratio in Eq. (20) must be of an order of 10^2 or 10^3 for low

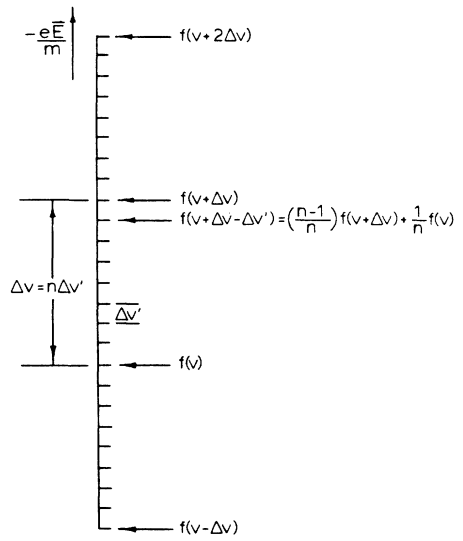

FIG. 3. Schematic representation of the acceleration procedure described in Eq. (19), showing the implementation of the Courant-Friedrichs-Lewy stability condition.

velocities in order to still be satisfied for high velocities. If the adiabatic condition, Eq. (20), is not met, an obvious consequence is that, if an array element of the collision term is negative, the corresponding array element of the resulting distribution function will become negative, yielding an unphysical result.

V. RESULTS AND DISCUSSION

The algorithm described in Sec. III was used to obtain the transient behavior of the EVDF and of various electron-swarm parameters for electrons in gaseous neon and gaseous argon. The swarm parameters under investigation were V_d, $\langle \varepsilon \rangle$, and R_i, which are the drift velocity, average energy of the electrons, and the ionization rate of the gas atoms, respectively. The time dependence of these quantities was calculated from the *normalized* velocity distribution function, which was obtained at each time step. The normalized distribution function $F(v,\psi,t)$ is defined as follows:

$$F(v,\psi,t) = \frac{f(v,\psi,t)}{A(t)} , \tag{21}$$

where

$$A(t) = 2\pi \int_0^\infty v^2 dv \int_0^\pi f(v,\psi,t)\sin\psi \, d\psi \tag{22}$$

and

$$A(0) \equiv 1 . \tag{23}$$

The various electron-swarm parameters are defined as follows:

$$R_i = 2\pi N \int_0^\pi v^2 dv \int_0^\pi v\sigma_{\text{ion}}(v) F(v,\psi,t)\sin\psi \, d\psi , \tag{24}$$

where $\sigma_{\text{ion}}(v)$ is the ionization cross section of the atoms by electron impact:

$$V_d = 2\pi \int_0^\infty v^2 dv \int_0^\pi v \cos\psi F(v,\psi,t)\sin\psi \, d\psi \ , \quad (25)$$

and

$$\langle \varepsilon \rangle = 2\pi \int_0^\infty v^2 dv \int_0^\pi \tfrac{1}{2} m v^2 F(v,\psi,t)\sin\psi \, d\psi \ . \quad (26)$$

By using a normalized distribution function, the total number of electrons in the distribution function is kept constant; this situation is analogous to a steady-state Townsend (SST) experiment. A pulsed Townsend (PT) experiment can be simulated by using an *unnormalized* time-evolved distribution function, since in such an experiment the number of electrons does not stay constant. In a PT calculation, the final equilibrium values of the swarm parameters, obtained from the unnormalized final equilibrium distribution function, will depend on the initial conditions. On the other hand, the equilibrium values of the swarm parameters in an SST calculation are independent of the initial conditions. For this reason, we have chosen to present only the normalized SST results for various swarm parameters. In each case a Maxwellian velocity distribution of electrons was assumed at time $t=0$ and a gas density N of 3.54×10^{16} cm^{-3} (1.32×10^{-3} amagat or, equivalently, 1 Torr at 273 K) was used. Isotropic scattering was assumed in all cases.

The convergence of the swarm parameters to their final equilibrium values occurs more quickly as the value of E/N becomes larger. For cases in which the E/N values are small, the time required to reach equilibrium can become large, forcing the calculation to consume more computing time. In cases of small E/N and when only the final equilibrium values of various swarm parameters are of interest, the time-*independent* two-term expansion methods may be computationally more efficient (although the time dependence will be lost). In cases of large E/N, however, convergence is fast enough so that the time-dependent calculations described in this paper become practical with very modest computing resources

A. Electrons in neon

For neon, the velocity steps Δv ranged from 2.05×10^7 to 3.40×10^7 cm/sec, and the time steps Δt ranged from 0.1 to 0.02 nsec as the E/N ratio was varied from 35 to 566 Td. The relevant scattering cross sections used in the calculations were taken from Ref. 2. Figure 4 displays the calculated time-dependent behavior of the electron-swarm parameters for $E/N=566$ Td and with initial average energies of 44 and 20 eV. From this figure, it is evident that, although the final equilibrium values of the swarm parameters are unaffected by the average energy value of the initial velocity distribution function, the transient behavior may be considerably different. For example, an overshoot in the drift velocity is observed if the initial average energy of the EVDF is less than the final equilibrium value, but the overshoot does not appear if the initial average energy is somewhat higher than the final value.

Figure 5 displays the time-dependent behavior of the electron-swarm parameters in gaseous neon with E/N ratios of 35 and 72 Td. The initial value of $\langle \varepsilon \rangle$ for the cases of 35 and 72 Td are 12 and 16 eV, respectively. For

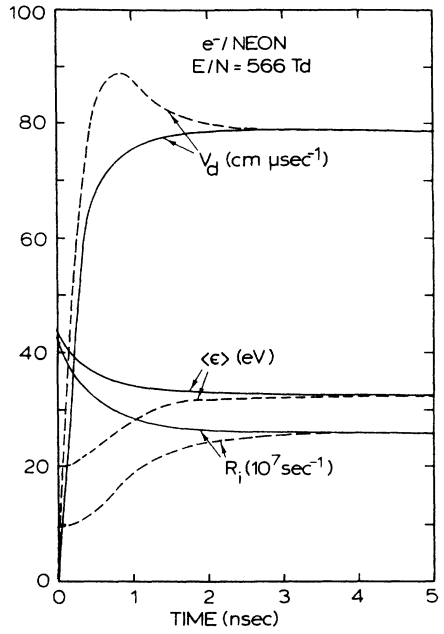

FIG. 4. Time dependence of various electron-swarm parameters in gaseous neon for $E/N=566$ Td. The data corresponding to the solid curves and the dashed curves have initial average electron energy of 44 and 20 eV, respectively.

the case in which $E/N=35$ Td, an overshoot of the drift velocity is present and slight undershoots of both the average energy and ionization rate can also be seen. The undershoots are not seen in the 72-Td data; however, a

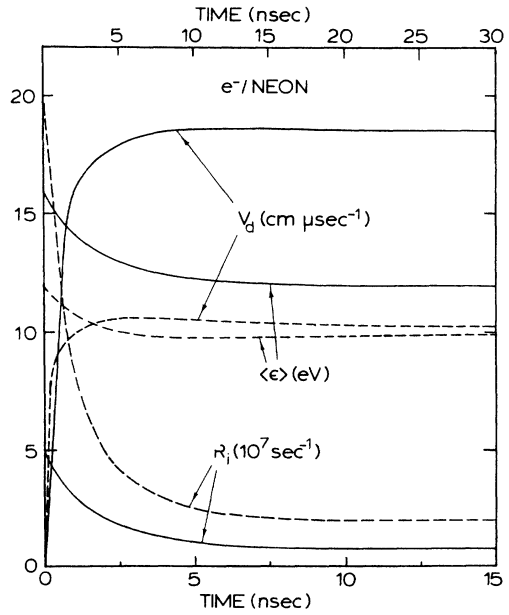

FIG. 5. Time dependence of various electron-swarm parameters in gaseous neon for $E/N=72$ Td (solid curves) and 35 Td (dashed curves). The upper and lower time scales correspond to the 35- and 72-Td data, respectively.

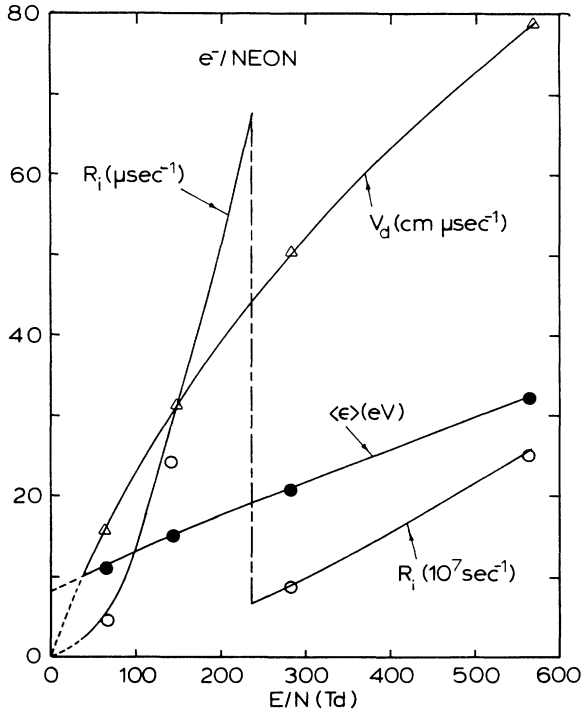

FIG. 6. Equilibrium values of various electron-swarm parameters in gaseous neon. The solid circles, open circles, and triangles are, respectively, the equilibrium values of $\langle \varepsilon \rangle$, R_i, and V_d from the calculations of Kitamori *et al.* (Ref. 2). The dashed lines for the values of E/N below 35 Td correspond to extrapolated values of various parameters.

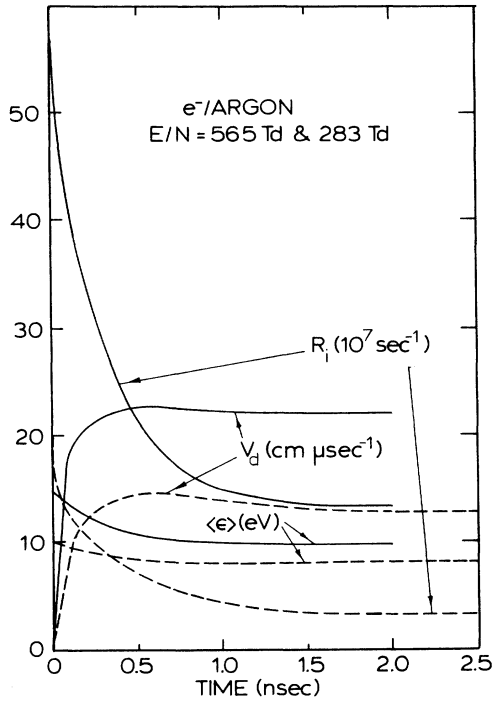

FIG. 7. Time dependence of various electron-swarm parameters in gaseous argon for $E/N = 565$ Td (solid curves) and 283 Td (dashed curves).

slight overshoot of the drift velocity is present. Whether or not these undershoots or overshoots occur depends on the initial value of the average energy of the swarm compared to that of the final equilibrium value. Recently observed[6,7] current overshoots in Ar-Hg and Ne-Hg discharges, and ionization rate overshoots in N_2 discharges, are presumably related to the initial conditions of the electron-energy distribution function.

The final equilibrium values of the electron-swarm parameters as a function of E/N are depicted in Fig. 6, and are in very good agreement with the values calculated by Kitamori, Tagashira, and Sakai.[2] The zero-field ($E/N = 0$) values of various parameters can be extrapolated from the curve of Fig. 6. These values are

$$V_d \rightarrow 0.0\text{cm/sec}, \quad R_i \rightarrow 0.0 \text{ sec}^{-1}, \quad \langle \varepsilon \rangle \rightarrow 8.7 \text{ eV} .$$

The variation in slope of the drift velocity, particularly near the lower E/N values, suggests that the electron mobility in neon, which is related to $\partial V_d/\partial(E/N)$, is slightly dependent upon E/N.

B. Electrons in argon

The cross sections for the elastic scattering of electrons with argon were taken from Massey and Burhop,[8] and the ionization cross sections were from Rapp and Englander-Golden.[9] The total excitation cross sections were adapted from Sakai *et al.*[10] by assuming a constant energy loss of 11.5 eV for all excitation processes.

Figures 7 and 8 display the time-dependent behavior of the electron-swarm parameters for E/N ratios ranging from 72 to 565 Td. For a given value of E/N, the velocity step Δv and time step Δt in the present case are comparable to those of the neon case. In each of these figures, overshoots in the drift velocities are observed and they are most dramatic when the initial average energy is

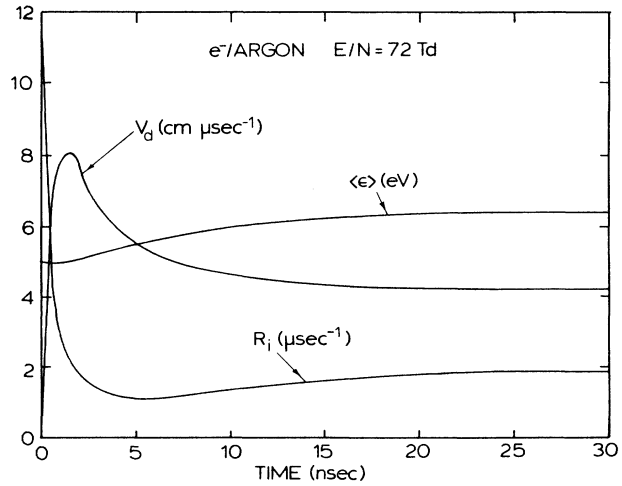

FIG. 8. Time dependence of various electron-swarm parameters in gaseous argon for $E/N = 72$ Td.

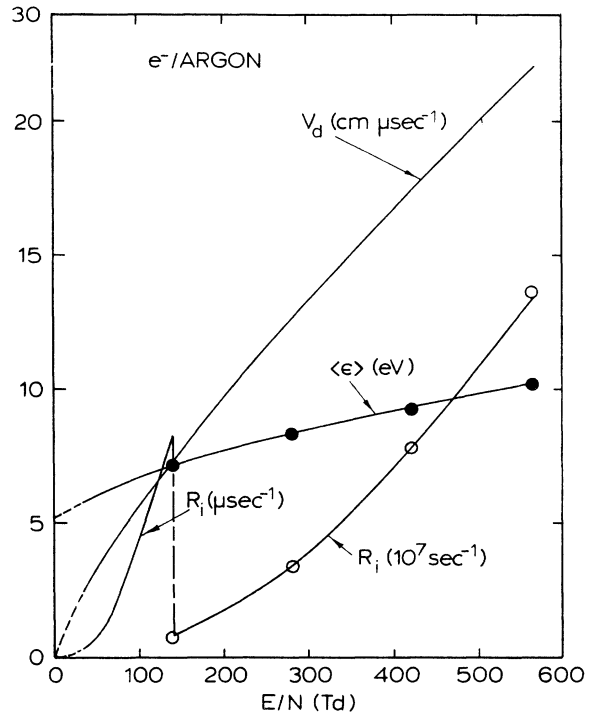

FIG. 9. Equilibrium values of various electron-swarm parameters in gaseous argon. The solid circles and the open circles are, respectively, the equilibrium values of $\langle \varepsilon \rangle$ and R_i from the SST calculations of Sakai *et al.* (Ref. 10).

closest to the final equilibrium average energy. That the size of the overshoot seems to vary inversely with the E/N ratio is merely an artifact resulting from the fact that the initial average energy values just happened to be chosen closer to the equilibrium values as the E/N ratios were reduced. In fact, the overshoot can be enhanced or completely eliminated at any E/N ratio by merely adjusting the value of the initial average energy.

Some preliminary analysis of the transient behavior of the presently calculated electron-swarm parameters (for both neon and argon) suggests that their time-dependent behavior can be accurately fitted by a sum of two exponentials. In fact, exponential behavior of the time dependence of various swarm parameters can be analytically justified,[11,12] especially for low values of E/N, by assuming a constant collision frequency which leads to a very simplified collision term.

The equilibrium values of the electron-swarm parameters in argon, plotted as a function of E/N, are shown in Fig. 9. As was done in the case of neon, the zero-field values of various swarm parameters can be obtained by extrapolation from this figure; this extrapolation procedure yields the following values:

$$V_d \rightarrow 0.0 \text{ cm/sec}, \quad R_i \rightarrow 0.0 \text{ sec}^{-1}, \quad \langle \varepsilon \rangle \rightarrow 5.2 \text{ eV} .$$

The equilibrium values in Fig. 9 can be compared with the values calculated by Sakai *et al.*[10] In their paper, various expressions used to define the drift velocity V_d were different from the expression used in the present calculations [Eq. (25)]. Thus meaningful comparisons could not be made for that parameter. The expressions for R_i and $\langle \varepsilon \rangle$ used in the SST condition calculations of Ref. 10 were equivalent to the expressions used in the present paper so that comparisons among these parameters are feasible. Figure 9 shows that the agreement between the two calculations is excellent.

The unnormalized equilibrium EVDF in argon is shown for two different values of E/N in Fig. 10. In both cases the initial distribution function (at $t=0$) is a spheri-

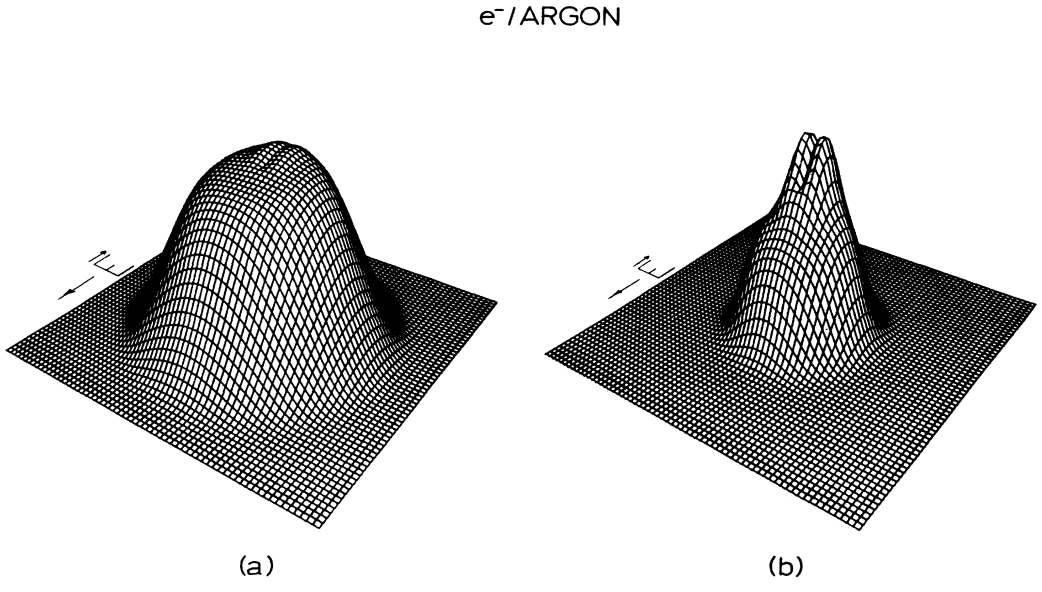

FIG. 10. Equilibrium velocity distribution function of electrons in argon for (a) $E/N=35$ Td and (b) $E/N=424$ Td.

cally symmetric Maxwellian with $\langle\varepsilon\rangle=5$ eV for $E/N=35$ Td and $\langle\varepsilon\rangle=30$ eV for $E/N=424$ Td. At equilibrium, the distribution function retains much of its spherical symmetry for low E/N. For large values of E/N, however, the equilibrium EVDF becomes highly asymmetric, suggesting that the effect of the electric field on the distribution function dominates over the effects of collisions. This clearly indicates that the two-term expansion procedure, which retains only first-order deviations from spherical symmetry, for obtaining the equilibrium EVDF, would be valid only for small values of E/N. The present procedure for obtaining the EVDF is valid for any value of E/N, small or large.

The "valley" near the origin ($v=0$) of the distribution function, which becomes very pronounced for large values of E/N, is probably due to the fact that very-low-energy electrons have a very small collision probability and are quickly accelerated by the electric field to a higher velocity where they become more likely to have collisions. On the other hand, the "upstream" electrons are not as efficiently accelerated into the origin (where they would replace those that have been accelerated out), because their velocities are already large enough so that they are inhibited by collisions.

VI. CONCLUSIONS

A very simple numerical algorithm has been described which obtains the time-dependent behavior of an electron-velocity distribution function in a gas. Aside from its simplicity, the algorithm has many unique and valuable features. Unlike many other methods of solution of the Boltzmann equation, the present method does not make use of any term expansions of the distribution function, and in this respect the solution is exact. The need for numerical evaluation of derivatives has been completely eliminated, which allows for a much more stable solution. The computational algorithm itself only involves summing and shifting of various array elements, which can be done without incurring any round-off error; this fact enhances the stability of the numerical procedure. Because of the simplicity of the procedure, the calculation can be performed with very modest computing resources. This is especially true in cases of high-E/N values for which convergence to equilibrium is much faster than for low E/N.

Although the calculations that are presented in this paper are for electron swarms in a pure gas, like neon or argon, subjected to a constant electric field, other more complicated situations can be very easily adapted to the present procedure. For instance, the present algorithm could be easily adapted to the case in which the electron swarm interacts with a gas mixture. Other situations of interest include the cases in which the projectile particles are more massive than electrons such as muons, protons, and heavy ions. Furthermore, the present procedure can easily accommodate the case in which the external electric field varies with time, such as an rf field. These other applications of the present procedure are under current investigation.

ACKNOWLEDGMENTS

It is a pleasure to thank Professor A. Garscadden for introducing us to this research problem and Professor H. H. Denman for valuable conversations. The support of the U.S. Air Force Office of Scientific Research through Grant No. AFOSR-87-0342 is gratefully acknowledged.

[1]A. V. Phelps and L. C. Pitchford, Phys. Rev. A **31**, 2932 (1985).
[2]K. Kitamori, H. Tagashira, and Y. Sakai, J. Phys. D **11**, 283 (1977).
[3]P. J. Drallos and J. M. Wadehra, J. Appl. Phys. **63**, 5601 (1988).
[4]T. Holstein, Phys. Rev. **70**, 367 (1946).
[5]R. Courant, K. Friedrichs, and H. Lewy, Math. Ann. **100**, 32 (1928).
[6]M. E. Duffy and J. H. Ingold, Bull. Am. Phys. Soc. **34**, 307 (1989).
[7]J. T. Verdeyen, L. C. Pitchford, Y. M. Li, J. B. Gerardo, and G. N. Hays, Bull. Am. Phys. Soc. **34**, 322 (1989).
[8]H. S. W. Massey and E. H. S. Burhop, *Electronic and Ionic Impact Phenomena*, 2nd ed. (Clarendon, Oxford, England, 1969), Vol. 1.
[9]D. Rapp and P. Englander-Golden, J. Chem. Phys. **43**, 1464 (1965).
[10]Y. Sakai, H. Tagashira, and S. Sakamoto, J. Phys. D **10**, 1035 (1977).
[11]B. Shizgal and D. R. A. McMahon, Phys. Rev. A **32**, 3669 (1985); D. R. A. McMahon, K. Ness, and B. Shizgal, J. Phys. B **19**, 2759 (1986).
[12]L. C. Pitchford, Air Force Wright Aeronautical Laoratory Technical Report No. AFWAL-TR-85-2106, 1985; G. N. Hays, L. C. Pitchford, J. B. Gerardo, J. T. Verdeyen, and Y. M. Li, Phys. Rev. A **36**, 2031 (1987).